



NUMERICAL SIMULATION OF LOW REYNOLDS NUMBER FLOWS OVER TWO CIRCULAR CYLINDERS IN TANDEM

Eric DIDIER^{1,2}

¹ Corresponding Author. Departamento de Engenharia Mecânica e Industrial, Faculdade de Ciências e Tecnologia, Universidade de Lisboa, 2829-516 Caparica, Portugal. Tel.: +351 21 294 85 67, Fax: +351 21 294 85 31, E-mail: deric@fct.unl.pt

² MARETEC, Instituto Superior Técnico, Technical University of Lisbon, Lisbon, Portugal.

ABSTRACT

Flow interference between two circular cylinders, with same diameter D , in tandem arrangement is investigated numerically using a fully coupled resolution method. Numerical simulations are performed for Reynolds number $Re=200$, with centre-to-centre cylinder distance L varying from 1.5 to $10D$. The two-dimensional Navier-Stokes equations are written in integral form and discretized by the finite volume method for unstructured grids. Equations are solved using an original fully coupled resolution method, without any transformation of continuity equation, that allows obtaining simultaneously velocity and pressure fields. Results analysis shows that change in flow topology occurs at $L=4D$ and manifests by a large jump on mean and fluctuating forces and Strouhal number. Similar trend is observed for present results at $Re=200$ and that obtained in a previous study at $Re=100$. It is show that maximum lift force is reached when vortex shedding of the two cylinders is in-phase and that forces acting on each cylinder are influenced by the phase lag of fluctuating lift between the two cylinders.

Keywords: finite volume, fully coupled resolution method, two tandem circular cylinders, unsteady flow, unstructured grid, vortex shedding

NOMENCLATURE

C_D	[-]	drag coefficient
C_L	[-]	lift coefficient
C_p	[-]	pressure coefficient
D	[m]	cylinder diameter
L	[m]	centre-to-centre distance between two cylinders
L_c	[m]	Critical spacing
L^*	[-]	normalized spacing, i.e. centre-to-centre distance between cylinders
Re	[-]	Reynolds number, $U_\infty D/\nu$
S	[-]	non-dimensional cell surface

St	[-]	Strouhal number, fD/U_∞
U_∞	[m/s]	free stream velocity
V	[-]	non-dimensional cell volume
f	[Hz]	frequency
n	[-]	interface normal vector
p	[-]	non-dimensional pressure
t	[-]	non-dimensional time
u	[-]	non-dimensional velocity
x_i	[-]	non-dimensional Cartesian co-ordinates

Φ [degree] phase lag

Subscripts and Superscripts

i	$i=1,2$; horizontal and vertical directions
o	reference values for a single cylinder
rms	root-mean-square value
–	time mean value

1. INTRODUCTION

Flow interference among pairs of circular cylinders with same diameter D in a tandem arrangement has been the subject of many investigations since this basic example of an array of multiple cylinders contributes to understand the interaction of multiple structures in a flow. The interference occurring in this type of arrangement causes significant changes in the parameters characterizing the aerodynamics of a single cylinder: average and fluctuating lift and drag forces, time average and fluctuating pressure distributions, Strouhal number and vortex shedding patterns. Obviously these changes are strongly influenced by centre-to-centre spacing, L , between the cylinders.

Many of the previous works regarding the flow around two circular cylinders were based primarily on flow visualization. These experimental investigations allowed identifying various interference regimes and authors, such as Igarashi [1], Zdravkovich [2, 3] and Sumner et al. [4], among others, proposed classifications of these regimes. According to the classification of Igarashi [1] six interference regimes can be identified for

tandem arrangement of circular cylinders: a) the free shear layers that originate from the separation of the upstream cylinder do not re-attach to the downstream cylinder; b) the shear layers that issue from the upstream cylinder are captured by the downstream one, but there is no vortex in between the cylinders; c) the shear layers that comes from the upstream cylinder are captured by the downstream one and symmetric vortices are formed between the cylinders; d) the vortices become instables; e) the shear layer emanating from the first cylinder roll up near the downstream cylinder; f) vortices shed off the front cylinder roll up before striking the rear cylinder and interact strongly with it.

The downstream cylinder is inside the near wake behind the upstream cylinder and therefore in a low momentum region. From regime a) to d) the mean drag of the downstream cylinder is small and negative and become positive for regime e) and f). The fluctuating forces are globally smaller than that of a cylinder before the critical distance, L_c . When vortices are shed from the upstream cylinder, after the critical distance, fluctuating lift and drag of the downstream cylinder became greater than of the upstream cylinder. The various studies showed the existence of the critical spacing between the cylinder, at $L_c/D=4.0$, that corresponds to a large jump in the fluctuating forces and Strouhal number. More recently, Alam et al. [5] show, for a sub-critical Reynolds number, that the phase lag between vortex shedding from two cylinders in tandem influences the forces acting on them and Assi et al. [6] analyse the unsteady response of circular cylinder under wake-induced excitation from a fixed upstream cylinder.

With the development of computational methods in fluids dynamics a better understanding of complex flows through numerical simulation became possible and detailed information has been obtained reproducing experimental studies. Following this trends, numerical investigations have been conducted by Li et al. [7], Slaouti and Stanby [8], Mittal et al. [9], Meneghini et al. [10], Sharman et al. [11], Carmo [12], and Carmo and Meneghini [13], among others. Recently Carmo et al. [14] investigated the effect of wake interference on flow-induced vibrations of circular cylinders in tandem. Different computational methods have been used, essentially for two-dimensional simulations at various Reynolds numbers, such as: vortex discrete method, finite volume method or spectral element method. Only Carmo and Meneghini [13] present a two- and three-dimensional study of flow around two cylinders in tandem, at Reynolds numbers, Re , between 160 and 320 using a spectral method. These authors found that, for $Re>190-200$, when three-dimensional structures are present in the flow field, a two-dimensional simulation is not sufficient to predict the parameters of aerodynamics

characteristics. However, even if two-dimensional computations are adapted for flow at $Re<190-200$, the various authors only studied some gaps and so doing estimated only roughly the critical distance. To the best of our knowledge, only Sharman et al. [11] published a more detailed numerical investigation for flow at $Re=100$, although not very detailed beyond the critical spacing. For large distance between the cylinders, computational cost increase drastically if a refined mesh is used.

Recently the present author published results of numerical investigation of flow interference between two circular cylinders in tandem at $Re=100$, Didier [15]. The author demonstrated that: i) forces acting on each cylinders are influenced by the phase lag of fluctuating lift between the cylinders; ii) fluctuating lift force acting on the downstream cylinder reaches its maximum for $L/D=5.25$ and not at the critical spacing, $L_c/D=4.0$, as observed at sub-critical Reynolds numbers [1-5].

The present study focuses on the flow interference considering cylinder spacing varying from $1.5D$ to $10.0D$, with a small spacing step in order to follow in detail the interaction between the cylinders and the flow. Flow simulations at Reynolds numbers 200 are carried out using an original fully coupled resolution method, without any transformation of continuity equation. This original method for solving the Navier-Stokes equations was developed by the author. Strouhal number, mean and fluctuating lift and drag, cross-correlation of fluctuating lift of each cylinder and the flow field patterns are analyzed. Details of the two-dimensional mechanism involved in the flow interference are presented and compared to that obtained previously for $Re=100$ by Didier [15] and literature results, from numerical simulations and experimental studies.

2. EQUATIONS

The governing equations for a Newtonian, incompressible viscous flow are the conservation of mass and the Navier-Stokes equations. In two-dimensions form and without body forces, they may be written as follows:

$$\frac{\partial u_i}{\partial x_i} = 0 \quad \text{with } i=1, 2 \quad (1)$$

$$\frac{\partial u_i}{\partial t} + u_j \frac{\partial u_i}{\partial x_j} = -\frac{\partial p}{\partial x_i} + \frac{1}{Re} \frac{\partial^2 u_i}{\partial x_j^2} \quad (2)$$

where u_i are the non-dimensional velocity components, p is the non-dimensional pressure, Re the Reynolds number.

On the circular cylinder surface a no-slip condition is applied, which implies that the fluid velocity is zero.

With the present formulation the velocity field is applied on the external boundary situated far from the cylinder.

$$u_1 = U_\infty, u_2 = 0 \quad (3)$$

3. NUMERICAL MODEL

3.1. Dimensionless integral equations

The unsteady bidimensional Navier-Stokes equations are written in conservative dimensionless integral form in the referential of the cylinder.

$$\int_S u_j n_j dS = 0 \quad (4)$$

$$\int_V \frac{\partial u_i}{\partial t} dV + \int_S u_i (u_j n_j) dS = - \int_V \frac{\partial p}{\partial x_i} dV + \frac{1}{Re} \int_S \frac{\partial u_i}{\partial x_j} n_j dS \quad (5)$$

where V is the volume of the element, S is its area and n_i the components of the outward unit vector normal to the surface.

3.2. Fully coupled resolution method

The present numerical code, developed by the author, solves the unsteady, incompressible and two-dimensional Navier-Stokes equations, without any transformation of the continuity equation. In the precedent version of the code, presented by Didier [15] and Didier and Borges [16, 17], a pressure equation has been reconstructed. In the present version of the numerical code, continuity equation is solved in its original form, without any transformation. A finite volume method with collocated cell-centred unknowns is used to discretize the equations for structured and/or unstructured grids.

Time-dependent solution of these equations requires using an implicit time-integration scheme. Momentum equations are integrated with a three-level second-order scheme. Spatial discretization schemes are implicit too. Diffusion terms are approximated by second-order central-differences scheme. Newton linearization is applied to convective terms. Velocities are approximated by the deferred correction method [18], using first-order UDS and third-order WACEB [19] schemes for the implicit and explicit part. Pressure at the midpoint face of the control volume is approximated by a second-order linear interpolation. For non-orthogonal grids, corrections are required to estimate velocity components and pressure to the face midpoint of the control volume.

The discretized continuity and momentum equations are gathered in one linear system and

solved simultaneously using the iterative algorithm Bi-CGSTAB- ω [20] with an incomplete LU preconditioning. The present resolution method does not require any dual-time scheme like in the artificial compressibility or pressure correction methods [21, 22], or any relaxation parameters.

Convergence study with mesh refinement, time step and outer boundary position was performed for $Re=100$ and $L/D=4.5$ by Didier [15]. It was show that acceptable convergence is obtained for a first grid point near to the wall at $e/D=0.8 \cdot 10^{-3}$, a non-dimensional time step equal to 10^{-2} and an outer boundary radius equal to $100D$. The same parameters are used for flow simulations at $Re=200$. Figure 1 shows the unstructured grid for $L/D=4.5$, composed by 51100 control volumes.

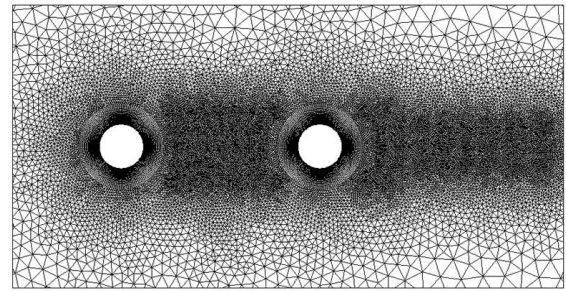


Figure 1. Unstructured grid for $L/D=4.5$

4. RESULTS AND DISCUSSION

The notations for two circular cylinders in tandem are show in Figure 2. The upstream and downstream cylinders are referenced as cylinder 1 and 2 respectively.

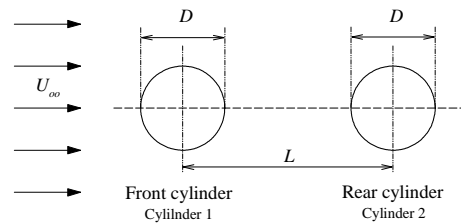


Figure 2. Notations for two cylinders in tandem

Flow around two cylinders in tandem with centre-to-centre distance, L , varying from $1.5D$ to $10.0D$ is simulated for Reynolds number $Re=200$. For these Reynolds numbers the flow is two-dimensional, as show numerically by Carmo [12] and Carmo and Meneghini [13].

Fundamental quantities for both cylinders are compared with that of a single one. For a single cylinder at $Re=200$, fundamental quantities are equals to 0.20 for the Strouhal number, 1.319 for the mean drag coefficient, 0.0287 and 0.455 for the drag and lift fluctuating coefficients.

4.1. Vortex shedding from the two cylinders

Figure 3 and 4 show the effect of the cylinders spacing on the Strouhal number, for $Re=100$ (from Didier [15]) and $Re=200$ respectively. The Strouhal number is defined as $St=fU_{\infty}/D$, where f is the dominant vortex shedding frequency. The frequency is calculated from a spectral analysis of

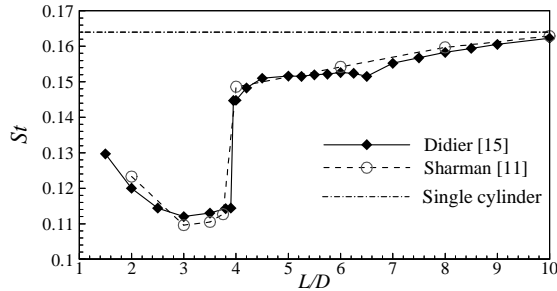


Figure 3. Strouhal number versus centre-to-centre distance L/D , $Re=100$ [15]

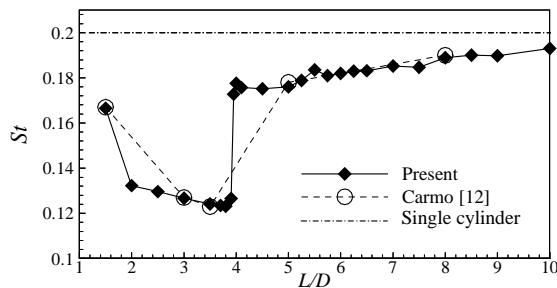


Figure 4. Strouhal number versus centre-to-centre distance L/D , $Re=200$

the fluctuating lift force acting on each cylinder using a Discrete Fourier Transform method.

The shedding frequency happens to be equal for both cylinders and all spacings. For $L < L_c$ upstream cylinder does not shed vortices. Nevertheless lift force acting on the upstream cylinder fluctuates with the frequency of the alternate shear layer that separates from the upstream cylinder and reattaches to the downstream one. Figure 5 show the time history of lift coefficient for each cylinders at $L/D=2.0$ and $Re=200$. Lift coefficient varies harmonically for the two cylinders. Lift frequency of upstream cylinder is the same that the lift frequency, i.e. vortex shedding frequency, of the downstream cylinder. Figure 6 shows the time history of lift coefficient for each cylinders, at $L/D=5.25$ and $Re=200$. In the co-shedding regime, for $L > L_c$, vortex shedding frequency from the downstream cylinder is identical to that from the upstream cylinder. Comparing time history of lift at $L/D=2.0$ and 5.25 , it can be observed that maximum lift coefficient in co-shedding regime is around ten times the maximum lift before L_c .

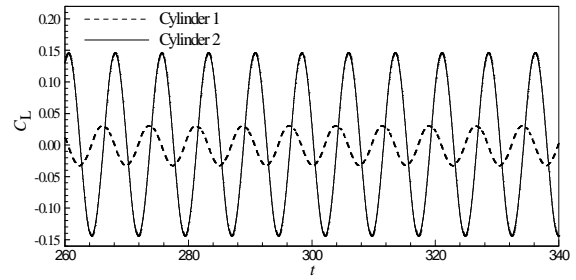


Figure 5. Lift coefficient history for rear and front cylinders at $L/D=2.0$ and $Re=200$

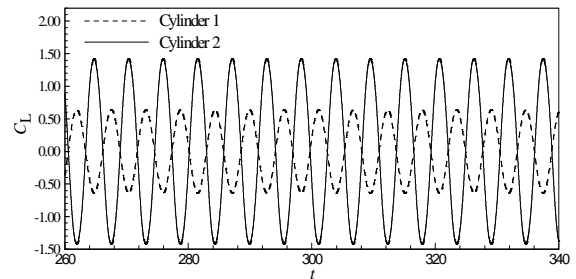


Figure 6. Lift coefficient history for rear and front cylinders at $L/D=5.25$ and $Re=200$

For the two Reynolds numbers, $Re=100$ and 200 , a similar behaviour is observed. The large jump in Strouhal number at $L/D=4.0$ corresponds to the critical spacing, where a bi-stable regime takes place. Before the critical spacing, Strouhal number decreases from the smaller spacing $L/D=1.5$ to $L/D=4.0$. Vortices are shed slowly at the rear cylinder. After the critical spacing, in the co-shedding regime, Strouhal number increases as L/D increases and tends to the Strouhal number of an isolated cylinder. However, Strouhal number increase is not regular. Fluctuations are observed for both Reynolds numbers: minimum and maximum fluctuations occur at different locations of L/D and depend of Reynolds number

Strouhal number, in Figures 3 and 4, is compared to other numerical results from Sharman [11] at $Re=100$ and from Carmo [12] at $Re=200$. A very good agreement is observed for the two Reynolds number flows between the present results and the two authors.

4.2. Time average drag forces

Figures 7 and 8 show the mean drag coefficient versus cylinder spacing for the two cylinders and Reynolds numbers $Re=100$ and 200 . The critical spacing is very apparent for the two Reynolds number flows and for the two cylinders. The mean drag coefficient is positive for the upstream cylinder and negative for the downstream cylinder for small spacing, less than the critical spacing. The effect is the manifestation of an attraction force between the cylinders. These results are in accordance with the

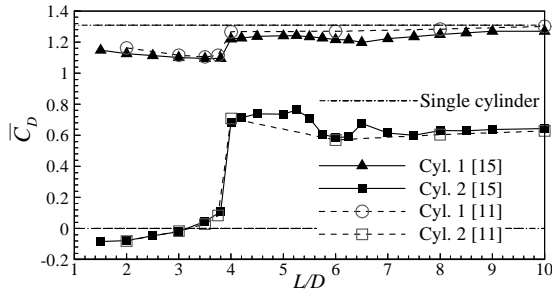


Figure 7. Mean drag coefficient versus centre-to-centre distance L/D , $Re=100$ [15]

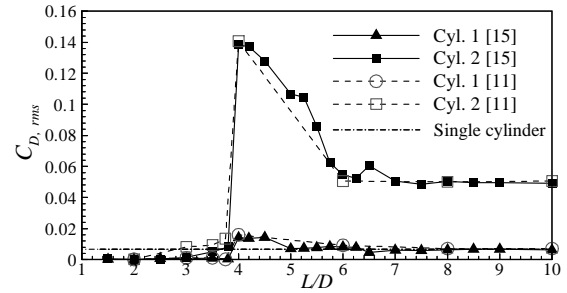


Figure 9. Fluctuating drag coefficient versus centre-to-centre distance L/D , $Re=100$ [15]

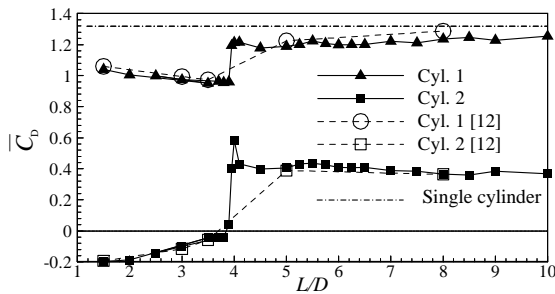


Figure 8. Mean drag coefficient versus centre-to-centre distance L/D , $Re=200$

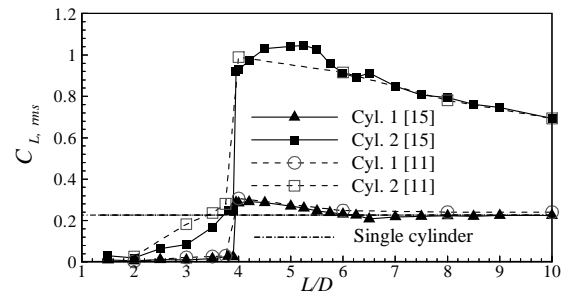


Figure 10. Fluctuating lift coefficient versus centre-to-centre distance L/D , $Re=100$ [15]

observation of Zdravkovich, in which a negative mean drag is observed for the same range of cylinder spacing. The mean drag coefficient on the downstream cylinder turns out to be less negative as the gap increases, and increases to small positive values and then jumps markedly at the critical spacing. The drag of cylinder 2 does not approach that of a single cylinder, even for large cylinder separations. Effectively, the downstream cylinder is immersed in the wake of the upstream cylinder, on a low momentum region. The presence of cylinder 2 also reduces the mean drag of cylinder 1, since it induces an increase in pressure in the separated wake behind the first cylinder.

Presents results of mean drag coefficient are compared with numerical results from Sharman et al. [11] at $Re=100$ and from Carmo [12] at $Re=200$. As for Strouhal number, a very good agreement is observed for the two Reynolds number flows between the present results and the two authors. The present numerical simulations, performed for several cylinder spacing in the co-shedding regime, show that mean drag presents an undulating variation with maximum and minimum values for both Reynolds number flows.

4.3. Fluctuating forces

Figures 9 and 10 show the fluctuating drag and lift for $Re=100$, from Didier [15], and Figures 11 and 12 shows the same fundamental quantities for $Re=200$. The fluctuating drag and lift coefficients follow similar trends to that of the mean drag coefficient as the cylinder spacing is increased.

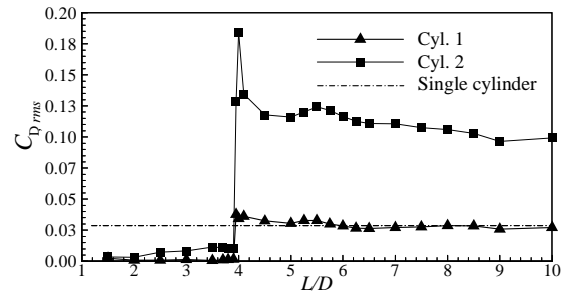


Figure 11. Fluctuating drag coefficient versus centre-to-centre distance L/D , $Re=200$

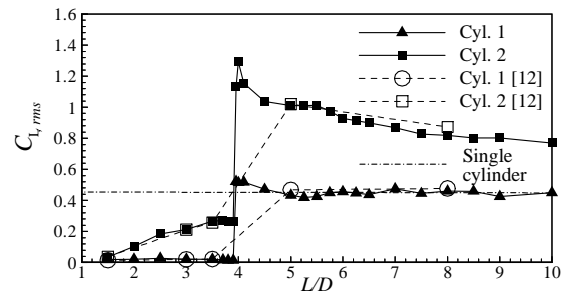


Figure 12. Fluctuating lift coefficient versus centre-to-centre distance L/D , $Re=200$

Fluctuations are small for sub-critical gap values. One can see that fluctuations on cylinder 1 remain extremely low. The fluctuations become larger as the cylinder spacing become superior to the critical spacing $L_c/D=4.0$. For the upstream cylinder, the fluctuations become slightly larger

than that of a single cylinder. However, for the downstream cylinder, the fluctuations become very large. The fluctuations are slowly reduced as the cylinder spacing is increased beyond the critical spacing.

However, fluctuating forces of downstream cylinder do not approach that of a single cylinder, even for large cylinder spacing. The downstream cylinder is immersed in the wake of the upstream cylinder which induces additional fluctuating forces to fluctuating forces due to the vortex shedding.

Current results are compared with those obtained by Sharman et al. [11], at $Re=100$, and Carmo [12], $Re=200$, and present an overall similar behaviour. Only a discrepancy for spacing near and slightly higher than the critical spacing are observed, certainly due to the use by Sharman et al. [11] of a medium mesh.

Present simulations performed for several spacing between the two cylinders, especially for the co-shedding regime, show interesting behaviour of fluctuating drag and lift for the two Reynolds numbers. As also observed previously for Strouhal number and mean drag coefficient, fluctuating forces present an undulating variation, more intense for the downstream cylinder than the upstream. The occurrence of maximum and minimum values of fluctuating lift is due, as it be discussed later, to synchronization of the wake behind the cylinders with in-phase and out-of-phase conditions, respectively. Sakamoto et al. [23] noted that, in case of two square cylinders, fluctuating lift becomes maximum at the critical spacing due to synchronization of the cylinders with a phase lag of 2π . Alam and Zhou [24], for sub-critical Reynolds number flow ($St \sim 0.2$), shows that maximum fluctuating lift, in the co-shedding regime, occurs at the critical spacing too. At $Re=200$, i.e. $St \sim 0.2$, maximum lift occurs also at the critical spacing.

It is also very interesting to note that lift behaviour for $Re=100$ and $Re=200$ is different, especially for the downstream cylinder. Even if lift coefficient is undulating for both Reynolds number flows, it can be observed that maximum of fluctuating lift coefficient of the downstream cylinder does not occur at the same spacing. For $Re=100$, maximum fluctuating lift is reached after the critical spacing, around $L/D=5.25$, but occur at the critical spacing for $Re=200$, as indicated before.

4.4. Phase lag of fluctuating lift

Synchronization of Strouhal number between the two cylinders occurred for both Reynolds numbers. Before the critical spacing, the dynamics in the near wake of the downstream cylinder and the shedding frequency are determined by the incident oscillatory flow. Figures 3 and 4 show that distribution of St is undulating and presents maximum and minimum values. Cross-correlation between the fluctuating lift forces of the two

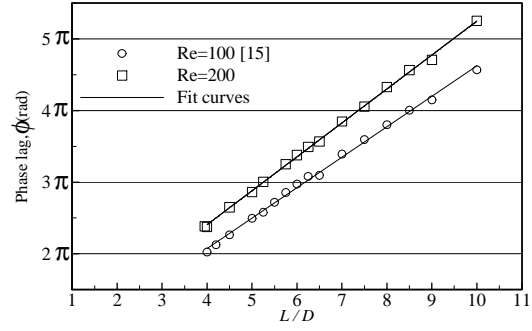


Figure 13. Variation of phase lag of fluctuating lift forces between the cylinders

cylinders demonstrates the existence of in-phase and out-of-phase situations, for both Reynolds numbers (Figure 13). Therefore, the interference between the bodies influences the resulting forces acting on the cylinders. Mean and fluctuating force present undulation associated to in- and out-of-phase configurations. These results indicate that proximity interference occurs between the cylinders. The downstream cylinder influences the resulting forces in the upstream one and vice versa. This suggests that vortex shedding from the upstream and downstream cylinder can be inhibited, in out-of-phase situation, or reinforced when in-phase configuration occurs, altering the forces acting on the two cylinders. Due to these interferences, the Strouhal number decreases with the diminution of the spacing between the cylinders.

As proposed by Alam and Zhou [24], the correlation between L/D and phase lag Φ can be obtained from curve-fits of the data for the two Reynolds number, $Re=100$ and 200 .

$$\phi = 0.4252 \pi L^* + 0.3715\pi, \text{ for } Re=100 \quad (6)$$

$$\phi = 0.4736 \pi L^* + 0.5121\pi, \text{ for } Re=200 \quad (7)$$

where $L^*=L/D$. The relations are valid for the co-shedding regime. With some modification of the relations and from the boundary conditions, $\Phi=2\pi$ at $L=L_c^*$, equations (6) and (7) may be rewritten as

$$\phi = 2.593 \pi St (L^*-L_c^*) + 2.073\pi \quad (8)$$

$$\phi = 2.368 \pi St (L^*-L_c^*) + 2.407\pi \quad (9)$$

Alam and Zhou [24] have proposed a general relation for the phase lag Φ obtained from curve-fits to data presented in their paper, considering various tandem arrangements of bluff bodies in a sub-critical regime:

$$\phi = 2.48 \pi St (L^*-L_c^*) + 2\pi \quad (10)$$

The relation ship (8) and (9) are similar to the general equation obtained by Alam and Zhou [24]. However discrepancy is noted for the slope value between the general equation and the relation

obtained for $Re=100$ and $Re=200$. That is probably due to the laminar nature of the flow in the present simulations. The results presented by Alam and Zhou in [24] are obtained in sub-critical regime.

4.5. Wake synchronization

In Figures 10 and 12 it can be seen that the fluctuating lift force does not necessary reach its maximum at the same spacing, as referred previously: at $Re=100$, the maximum occurs at $L/D=5.25$ whereas it is reached at $L/D=4.0$, the critical gap, at $Re=200$. The Strouhal number can be expressed as $St=D/\lambda$, with λ the characteristic length between a vortices pair [15]. For a single cylinder in a uniform flow, the Strouhal number at $Re=100$ and $Re=200$ is $St_{Re=100}=0.164$ and $St_{Re=200}=0.2$ respectively. Therefore, considering a cylinder diameter $D=1.0$, the characteristic length for each of these Reynolds number flows are $\lambda_{Re=100}=6.25$ and $\lambda_{Re=200}=5.00$. These length correspond to the distance between the downstream and upstream stagnation points of the cylinders, when the spacing is $L/D_{Re=100}=5.25$ and $L/D_{Re=200}=4.0$, when the fluctuating lift force reaches its maximum. Therefore a spatial synchronization is identified in addition to the in- and out- phase phenomenon. For a Strouhal number, a particular spacing exists where vortices shed from the upstream cylinder add to the vortices shed from the downstream cylinder, in a way that fluctuating lift forces reaches its maximum.

4.6. Flow topology

Figures 14 and 15 show the streamlines past the cylinders for $L/D=5.25$. Vortex shedding occurs from both cylinders. The binary wake is formed by the combination of one vortex shed from the cylinder 1 and another by cylinder 2. This effect contributes to large lift forces observed on the downstream cylinder. The binary wake is more intense at $Re=200$ than $Re=100$.

5. SUMMARY

Flow interference between two circular cylinders, with same diameter D , in tandem arrangement is investigated numerically using an original fully coupled resolution method, without any transformation of continuity equation, for solving the two-dimensional Navier-Stokes equations.

Numerical simulations are performed for Reynolds number $Re=200$, with centre-to-centre cylinder distance L varying from 1.5 to $10D$, with a small spacing step in order to follow in detail the interaction between the cylinders and the flow. Results at $Re=100$ are also presented for analysing low Reynolds number flows past two cylinders in tandem.

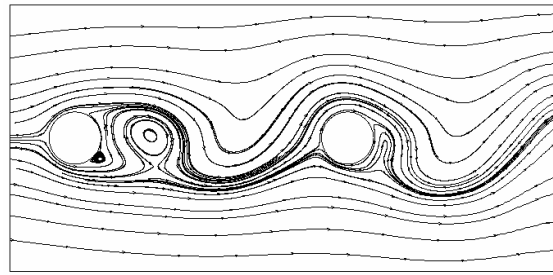


Figure 14. Streamlines for $L/D=5.25$ and $Re=100$

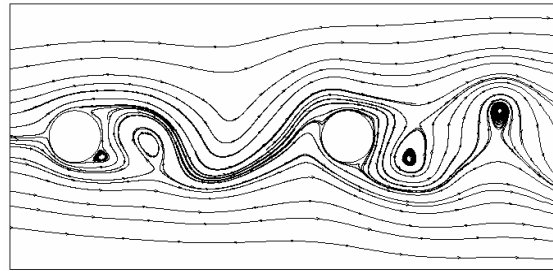


Figure 15. Streamlines for $L/D=5.25$ and $Re=200$

Present results, obtained at $Re=100$ and $Re=200$, agree very well with numerical results of Sharman et al. and Carmo, respectively.

As expected, change in flow topology occurs at $L=4D$ and manifests by a large jump on mean and fluctuating forces and Strouhal number, as observed for sub-critical regime.

The small spacing step used to increase centre-to-centre cylinder distance allows showing that maximum lift force is reached when vortex shedding of the two cylinders is in synchronization, i.e. for $L/D=5.25$ at $Re=100$ and $L/D=4.0$ at $Re=200$. Vortices shed from the upstream cylinder add to the vortices shed from the downstream cylinder, in a way that fluctuating lift forces reaches its maximum.

Mean and fluctuating forces and Strouhal number shows an undulating behaviour, with maximum and minimum values. Cross-correlation between the fluctuating lift forces of the two cylinders demonstrates the existence of in-phase and out-of-phase situations. Therefore, the interference between the cylinders influences the resulting forces acting on the cylinders and fluctuating lift force presents undulation associated to in-phase and out-of- phase of the flow pattern. Same results are obtained experimentally by Alam and Zhou for several bluff bodies in tandem in sub-critical regime.

REFERENCES

- [1] Igarashi, T., 1977, "Characteristics of the flow around two circular cylinders arranged in tandem", Bulletin of JSME, Vol. 24(188), pp. 323-331.

- [2] Zdravkovich, M.M., 1977, "Review of flow interference between two circular cylinders in various arrangements", *ASME Journal of Fluids Engineering*, Vol. 99, pp. 618-633.
- [3] Zdravkovich, M.M., 1987, "The effects of interference between circular cylinders in cross flow", *Journal of Fluids and Structures*, Vol. 1, pp. 618-633.
- [4] Sumner, D., Price, S.J., and Païdoussis, M.P., 2000, "Flow-pattern identification for two-staggered circular cylinders in cross-flow", *Journal of Fluid Mechanics*, Vol. 411, pp. 263-303.
- [5] Alam, M.M., Moriya, M., Takai, K., and Sakamoto, H., 2003, "Fluctuating fluid forces acting on two circular cylinders in a tandem arrangement at a subcritical Reynolds number", *J. Wind Eng. Ind. Aerodyn.*, Vol. 91, pp. 139-154.
- [6] Assi, G., and Bearman, P., 2008, "Unsteady response of a circular cylinder under wake-induced excitation from a fixed upstream cylinder", *Proc. Conf. On Flow Induced Vibration*, Zolotarev and Horacek eds., Institute of Thermomechanics, Prague, pp. 787-792.
- [7] Li, J., Chambarel, A., Donneaud, M., and Martin, R., 1991, "Numerical study of laminar flow past one and two circular cylinders", *Comput. Fluids*, Vol. 19, pp. 155-170.
- [8] Slaouti, A., and Stansby, P.K., 1992, "Flow around two circular cylinders by the random-vortex method", *Journal of Fluids and Structures*, Vol. 6, pp. 641-670.
- [9] Mittal, S., Kumar, V., and Raghuvanshi, A., 1997, "Unsteady incompressible flows past two cylinders in tandem and staggered arrangements", *Int. J. Numer. Meth. Fluids*, Vol. 25, pp. 1315-1344.
- [10] Meneghini, J.R., Saltara, F., Siqueira, C.L., and Ferrari, J.A., 2001, "Numerical simulation of flow interference between two circular cylinders in tandem and side by side arrangements", *J. Fluids and Structures*, Vol. 15, pp. 327-350.
- [11] Sharman, B., Lien, F.S., Davidson, L., and Norberg, C., 2005, "Numerical predictions of low Reynolds number flows over two tandem circular cylinders", *Int. J. Numer. Meth. Fluids*, Vol. 47, pp. 423-447.
- [12] Carmo, B.S., 2005, "Estudo numérico do escoamento ao redor de cilindros alinhados". Master Thesis, Escola Politécnica da Universidade de São Paulo, Brasil.
- [13] Carmo, B.S., and Meneghini, J.R., 2006, "Numerical investigation of the flow around two circular cylinders in tandem", *Journal of Fluids and Structures*, Vol. 22, pp. 979-988.
- [14] Carmo, B., Sherwin, S., and Bearman, P., 2008, "Numerical simulation of the flow-induced vibration in the flow around two circular cylinders in tandem arrangements", *Proc. Conf. On Flow Induced Vibration*, Zolotarev and Horacek eds., Institute of Thermomechanics, Prague, pp. 787-792.
- [15] Didier, E., 2007, "Flow simulation over two circular cylinders in tandem", *C. R. Mécanique*, Vol. 335, pp. 696-701.
- [16] Didier, E., and Borges, A.R.J., 2003, "Unsteady Navier-Stokes equations: A fully coupled method for unstructured mesh", *Proc. Conference on Modelling Fluid Flow*, pp. 814-821, Budapest, Hungary.
- [17] Didier, E., and Borges, A.R.J., 2007, "Numerical predictions of low Reynolds number flow over an oscillating circular cylinder", *Journal of Computational and Applied Mechanics*, Vol. 8(1), pp. 39-55.
- [18] Khosla, P., and Rubin, S., 1974, "A diagonally dominant second-order accurate implicit scheme", *Comput. Fluids*, Vol. 2, pp. 207-209.
- [19] Song, B., Liu, G.R., Lam, K.Y., and Amano, R.S., 2000, "On a higher-order bounded discretization scheme", *Int. J. Numer. Meth. Fluids*, Vol. 32, pp. 881-897.
- [20] Sleijpen, G.L.G., and van der Vorst, H.A., 1995, "Maintaining convergence properties of BiCGSTAB methods in finite precision arithmetic", *Numer. Algorithms*, pp. 203-223.
- [21] Issa, R.I., 1985, "Solution of the implicit discretized fluid flow equations by operator-splitting", *J. Comp. Physics*, pp. 40-65.
- [22] Prakash, C., and Patankar, S.V., 1985, "A control-volume-based finite-element method for solving the Navier-Stokes equations using equal-order velocity-pressure interpolation", *Num. Heat. Transfer*, Vol. 8, 259-280.
- [23] Sakamoto, H., Haniu, H., and Obata, Y., 1987, "Fluctuating forces acting on two square prisms in a tandem arrangement", *J. Wind Eng. Ind. Aerodyn.*, Vol. 26, pp. 85-103.
- [24] Alam, M.M., and Zhou, Y., 2007, "Phase between vortex shedding from two tandem bluff bodies", *Journal of Fluids and Structures*, Vol. 23, pp. 339-347.